Indian Journal of Chemical Technology
Vol. 24, March 2017, pp.169-177

Anti-corrosive properties of 2, 3-dihydroxyquinoxaline on mild steel corrosion in sulphuric acid

Kirti Kansal, Rashi Chopra, Raman Kumar, Akshay Kumar, Bhaskaran Yadav, Raj Kishore Sharma & Gurmeet Singh*

Department of Chemistry, University of Delhi, Delhi 110 007, India
E-mail: gurmeet123@yahoo.com

Received 9 April 2016; accepted 29 December 2016

2, 3-Dihydroxyquinoxaline (DHQ) has been investigated as an inhibitor for mild steel corrosion in 0.5 MH_2SO_4 solution using electrochemical techniques [Galvanostatic polarization, Potentiostatic polarization and electrochemical impedance spectroscopy (EIS)] and non-electrochemical technique (weight loss). It has been found that the inhibition efficiency of the inhibitor increases with increase in concentration. The effect of temperature ranging from 298 K to 328 K on the corrosion rate have been studied and various thermodynamic parameters are calculated. Polarization studies show that investigated inhibitor is of mixed type in nature and shows a passive range at 298 K. The adsorption of the inhibitor on the mild steel surface in acid solution is found to obey the Langmuir adsorption isotherm. Scanning electron microscopy (SEM) and Atomic Force microscopy (AFM) are performed on inhibited and uninhibited mild steel samples to analyze the surface morphology and topography. Quantum chemical calculations have also employed using the semi empirical AM1 method for theoretical calculations and obtained results are found to be in good agreement with the experimental findings.

Keywords: AFM, DHQ, Electrochemical impedance spectroscopy, Mild steel, Polarization, Quantum, SEM, Weight loss.

Mild steel, an alloy of iron is widely used as main construction material in many industries due to its excellent mechanical properties and low cost. Acidic solutions are predominantly used in chemical laboratories, and for industrial processes such as acid pickeling, acid cleaning, acid-descaling and oil-well acidizing[1]. Sulphuric acid is extensively used in such processes which results in corrosive attack of metal causing huge economic loss[2]. Thus to restrain destructive corrosion attack of acid environment on metallic materials, inhibitors are used as one of the most practical and efficient methods available[3-7]. The selection of inhibitor is controlled by its cost, toxicity, economic availability, its efficiency to inhibit the metal surface and its environment friendliness[8]. Organic compounds containing heteroatom's with high electron density such as oxygen, sulphur, nitrogen atoms and multiple bonds which act as adsorption centers in the molecule are effective corrosion inhibitors[9].

2, 3-Dihydroxyquinoxaline (DHQ) is a non toxic, commercially available heterocyclic aromatic organic compound containing π electrons and two nitrogen atoms and two hydroxyl groups, which induces a greater extent of adsorption of inhibitor molecule onto the surface of mild steel as compared to one nitrogen atom or oxygen atom containing heterocyclic compounds. Experimental works have suggested that quinoxaline and its derivatives are non-toxic environmentally acceptable inhibitors for mild steel, copper and carbon steel in acidic medium[9-19]. The aim of present work was to study the effect of DHQ as an inhibitor for mild steel in 0.5M H_2SO_4 medium using electrochemical (galvanostatic polarization, potentiostatic polarization and electrochemical impedance spectroscopy) and non- electrochemical (weight loss) techniques. The study was also complemented by quantum chemical calculations and surface morphological studies.

Experimental Section

DHQ was purchased commercially from Alfa Aesar with 99% purity. The inhibitor solution used was made of AR grade H_2SO_4, appropriate concentration of acid was prepared using tripled distilled water. The concentration range of the inhibitor employed was 10^{-2} to 10^{-5}M.

Mild steel encapsulated in a Teflon holder with area of 1 cm^2 (composition in percentage C = 0.15, Si = 0.08, S = 0.025, Mn = 1.02 and Fe = 98.725) was used for this study as working electrode. The samples were polished using SiC abrasive papers of different grades (from 100 to 2000). The electrode potentials

were measured with respect to saturated calomel electrode as reference electrode and platinum wire as auxiliary electrode at 298 K, 308 K, 318 K and 328 K.

For weight loss measurements, mild steel specimens (1cm×1cm×1cm) were immersed in 0.5 M H_2SO_4 and 10^{-2} and 10^{-5} M inhibitor concentration for 6 h at room temperature. Then the specimens were removed, rinsed in distilled water, acetone and the loss in weight of the specimen was determined.

All the electrochemical measurements were performed using electrochemical work station (Model No: CHI 760D, CH Instruments, USA). For electrochemical studies three electrodes cell assembly containing the grinded and polished working electrode was kept immersed in the test solution for 2 h until a steady state of open circuit potential (OCP) is reached. Galvanostatic measurements were taken in the presence and absence of inhibitor at different concentrations from a potential range of -500 to 2000 mV. The corrosion characteristics such as corrosion potential (E_{corr}), corrosion current density (I_{corr}) and anodic (β_a)/cathodic (β_c) Tafel slopes were obtained from the software installed in the instrument. The electrode system is same for potentiostatic polarization studies as that of galvanostatic polarization studies. A pre-determined potential was given and corresponding current values were recorded at the scanning rate of 0.1 mV/s.

For EIS measurements a small alternating voltage perturbation (0.005V) was imposed on the cell over the frequency range 1Hz to 100 KHz as open circuit potential (OCP) is reached. The inhibition efficiency (Θ_{EIS}) and the double layer capacitance (C_{dl}) calculated from the values of charge transfer resistance (R_{ct}) and frequency at maximum imaginary component of the impedance (f_{max}). The Nyquist and Bode Plots were obtained from the measurements.

Morphology of metal surface was studies using scanning electron microscope model (SEM-JSM-6610LV). The specimens used for SEM were grinded mild steel specimens immersed in the 0.5 M H_2SO_4 with and without inhibitor DHQ for 24 h.

AFM (Model:NanosurfNaio) was done to further analyze the surface morphology of the uninhibited and inhibited mild steel surfaces so as to provide quantitative information about the surface roughness. A contact mode atomic force microscope with a Si_3N_4 cantilever (Nanosensor, CONTR type) having a spring constant of 0.1 N m^{-1} and tip radius more than 10 nm was used to calculate roughness of the surfaces.

Quantum chemical calculations for DHQ was carried out using AM1 semi-empirical molecular orbital method in Hyperchem version 8.0, a quantum mechanical program marketed by Hypercube, Inc.. Geometry optimization was done and calculations of molecular energies followed by values of various quantum descriptors were done.

Results and Discussion

Weight loss studies

Weight loss one of the most fundamental techniques of corrosion science measures mass change (weight loss or weight gain) of test specimens to evaluate material degradation as function of exposure time or temperatures in corrosive environments[20]. Weight loss of mild steel specimens was determined in 0.5 M H_2SO_4 solution, in 10^{-2} M and 10^{-5} M DHQ solution respectively after immersion of 6 h at 298K. The corrosion rate and inhibition efficiencies in the presence of the inhibitor for mild steel specimens are shown in Table 1 were calculated using the following Equation:

$$IE\,\% = \frac{Wo - Wi}{Wo} \times 100$$

where, W_o and W_i (in g) are the values of the weight loss observed of mild steel in absence and presence of inhibitor, respectively[21].

The data depicts that with increase of weight loss of mild steel in the acid, inhibition efficiencies decreases with decreasing concentration of inhibitor. The decrease in the inhibition efficiency can be attributed to the decrease of both the adsorption amount and the coverage of inhibitor on metal surface with the decrease of inhibitor concentration[22,23].

Galvanostatic studies

Polarization profiles for mild steel in 0.5 M H_2SO_4 in the absence and presence of DHQ of various concentrations at 298 K is shown in Fig. 1. The values of various parameters and inhibition efficiency values I.E. (%) calculated from curves obtained at various temperatures i.e. 298 K, 308 K, 318 K, and 328 K are listed in Table 2 using the following equation:

Table 1 — Weight loss measurement for DHQ at 298 K.

Concentration (M)	(W_0)/g	(W_i)/g	I.E.%
10^{-2} M DHQ	1.0406	0.066	93.65
10^{-5} M DHQ	1.0406	0.364	65.02
0.5 M H_2SO_4	1.0406	-	-

$$\text{I.E.}(\%) = \frac{I_{Corr} - I_{inh}}{I_{Corr}} \times 100$$

where, I_{corr} and I_{inh} are the corrosion current densities without and with the addition of various concentrations of the inhibitor[24].

From the experimental data, we observed that the corrosion rate or current density i.e. I_{corr} values increase with increase in temperature and thus I.E. decrease with increase in temperature. Also data suggests that DHQ behaves as a good corrosion inhibitor as I_{corr} is decreased which results in increase of I.E. with increase in inhibitor concentration. As it can be seen from Table 2 that there is no appreciable shift in corrosion potential (E_{corr}) values it can be concluded that the inhibitor shows mixed type behaviour and suppresses both anodic and cathodic reaction by adsorption on steel surface[25].

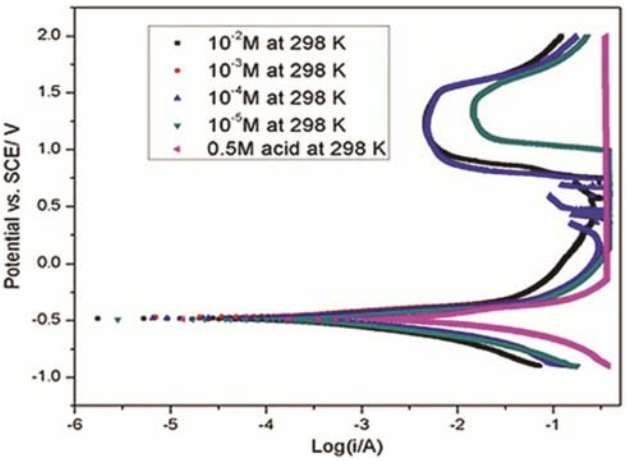

Fig. 1 — Tafel curves for mild steel in 0.5 M H_2SO_4 containing different concentration of DHQ at 298K.

Potentiostatic polarization studies

Passivity effect the kinetics of the corrosion process because of the formation of the protective film which acts as a barrier to attack on the mild steel surface environment[26]. The potentiostatic polarization studies of mild steel in the 0.5 M H_2SO_4 in the presence of DHQ was carried out at 298 K and the polarization curves so obtained containing various concentrations of DHQ are shown in Fig. 2. The effect of addition of DHQ was studied in the terms of the electrochemical parameters like critical current (i_c), passive current (i_p), and Flade potential (E_{pp}) which are tabulated in Table 3. The potentiostatic range in the Tafel plot (i.e. from -500 mV to 2000 mV) reveals that a passive range is observed for all concentrations of DHQ at 298 K indicating that in this range the inhibitor forms a protective film that acts as a barrier to attack on the metal surface by the

Table 2 — Galvanostatic polarization parameters for the corrosion of mild steel in 0.5 M H_2SO_4 containing different concentration of DHQ.

Temp. (K)	Conc. (M)	$-E_{corr}$ (mV vs. SCE)	b_c (mV/decade)	b_a (mV/decade)	I_{corr} (mA cm^{-2})	I.E. (%)
298	10^{-2}	447	128.23	29.30	0.0435	98.94
	10^{-3}	487	114.78	33.56	0.0636	98.4
	10^{-4}	487	102.79	70.83	0.6353	84.63
	10^{-5}	477	102.02	78.65	1.096	73.48
	0	489	119.26	99.33	4.134	-
308	10^{-2}	480	137.04	143.163	0.2101	97.47
	10^{-3}	508	121.32	74.101	0.2662	96.8
	10^{-4}	482	116.97	79.02	1.393	83.28
	10^{-5}	494	133.83	110.265	3.622	56.54
	0	514	154.70	155.11	8.336	-
318	10^{-2}	501	142.22	179.11	0.4523	96.52
	10^{-3}	498	147.12	201.81	1.004	92.28
	10^{-4}	487	138.54	84.82	6.063	53.39
	10^{-5}	502	168.66	169.69	7.418	42.98
	0	480	174.97	164.88	13.01	-
328	10^{-2}	493	107.04	83.90	0.7182	95.34
	10^{-3}	490	147.53	151.653	1.479	90.41
	10^{-4}	477	144.30	79.64	7.44	51.78
	10^{-5}	476	149.25	96.64	9.35	39.4
	0	480	177.65	150.30	15.43	-

environment leading to passivation[27]. But no such passivation was observed at higher temperatures. This can be due to the desorption of inhibitor at higher temperatures. Also it can be seen that passivation potential range is increasing with increase of inhibitor concentration indicating good passivity at higher concentrations of DHQ. The critical current density values are found to be lower in the presence of additives as compared to acid alone; suggesting thereby that these additives are adsorbed on the metal surface.

Electrochemical impedance studies

The corrosion inhibition of the mild steel specimens in 0.5 M H_2SO_4 containing different concentrations of inhibitor solution were carried out using EIS measurements at different temperatures and the Nyquist and Bode plots are shown in Figs 3 and 4. The Nyquist plot clearly indicates that the diameter increases with increasing inhibitor concentration indicating that charge transfer process is mainly controlling the corrosion process for mild steel. The inhibition efficiency (Θ_{EIS}) calculated from the values of charge transfer resistance (R_{ct}) using the following Equation:

$$\theta EIS = \frac{Rct^{o} - Rct}{Rct^{o}} \times 100$$

where, $R_{ct}°$ and R_{ct} are the charge transfer resistance values in the presence and absence of the inhibitor, respectively[28]. The double layer capacitance (C_{dl}) was calculated from the following Equation:

$$C_{dl} = \frac{1}{2 \quad f max Rct}$$

where, f_{max} is the frequency at maximum imaginary component of the impedance[28]. The C_{dl} values as

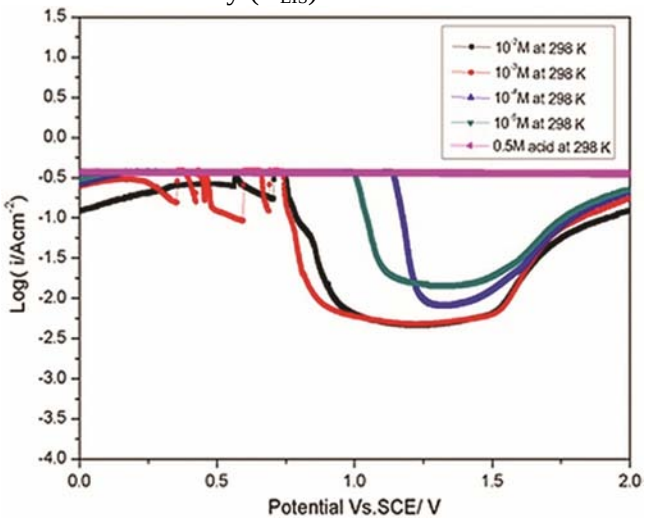

Fig. 2 — Passive range curves for mild steel in 0.5 M H_2SO_4 containing different concentration of DHQ at 298 K

Table 3 — Potentiostatic polarization parameters for the corrosion of mild steel in 0.5 M H_2SO_4 containing different concentration of DHQ at 298 K.

Conc. (M)	I_c (mA cm^{-2})	I_{pp} (mA cm^{-2})	E_{pp} range (mV)
10^{-2}	353	16.87	882 – 1560
10^{-3}	384	16.14	886 – 1561
10^{-4}	387	41.00	1187– 1545
10^{-5}	369	47.20	1069– 1571
0	345	-	-

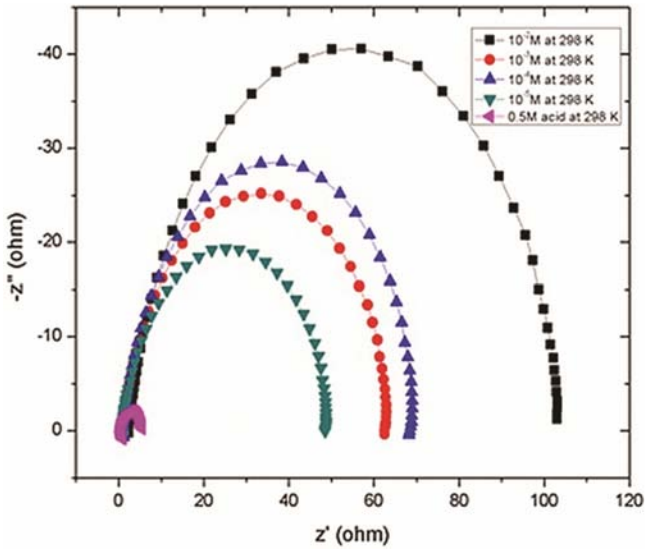

Fig. 3 — Complex-Plane impedance (Nyquist Plot) of mild steel in 0.5 M H_2SO_4 at 298 K in the presence of various concentrations of DHQ

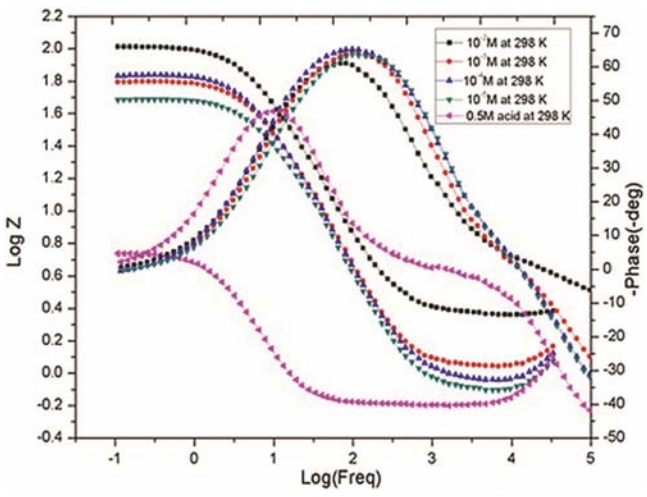

Fig. 4 — Bode plot for various concentration of DHQ at 298 K

listed in Table 4 decreases with increase in the inhibitor concentration which can be attributed to a decrease in local dielectric constant and an increase in thickness of electric double layer. This suggests that inhibitor molecules inhibit the corrosion rate by adsorption at metal/solution interface[29]. The Bode plots (Fig. 4) shows an increase of absolute impedance at low frequencies confirming the higher protection of mild steel with increase in the concentration of DHQ on mild steel surface[30]. In the same graph, phase angle plots depicted evidently that with increasing the concentration of DHQ in the investigated solution, the phase angle shifts to more negative values and closer to 90° indicating superior inhibitive behaviour due to the adsorption of the metal surface of more inhibitor molecules at higher concentrations[31].

Adsorption isotherm and Free energy of adsorption

The mechanism of adsorption and the surface behaviour of various organic molecules can be easily viewed through adsorption isotherms. Different adsorption isotherms were considered namely Langmuir, Temkin, Frumkin, El-awady, Flory huggins and Freundlich isotherms. The various thermodynamic parameters can be evaluated by determining the best fit isotherm with the aid of correlation coefficient (R^2). Among the above mentioned isotherms the best fit isotherm for adsorption of DHQ was Langmuir isotherm and is expressed as[32]:

$$\frac{C_{inh}}{\theta} = \frac{1}{K} + C_{inh}$$

where, C_{inh} is the concentration of the inhibitor, K is the equilibrium constant for the adsorption process and Θ is the degree of the surface coverage which is calculated as:

Θ = (I.E. %) /100

The plot between C_{inh}/Θ versus C_{inh} gives a straight line with intercept 1/K (Fig. 5). The value of adsorption equilibrium constant K is related to standard Gibb's free energy by:

$$\Delta G°_{ads} = -RT\ln(55.5\ K)$$

where, 55.5 is the molar concentration of water, R is the universal gas constant and T is the absolute temperature in Kelvin[33].

The thermodynamic data obtained from adsorption isotherm is tabulated in Table 5. A high K_{ads} value indicates that the inhibitor is strongly adsorbed on the metal surface reflecting the increasing adsorption capability due to structural formation on the metal surface[34]. Negative value of $\Delta G°_{ads}$ indicates that the adsorption process for DHQ is spontaneous in nature[35].

The values of $\Delta G°_{ads}$ obtained for the inhibitor in acidic solution are close to -40 kJ/mol, indicating predominantly chemisorption[36].

A plot of log K versus 1/T in Fig. 6 was used to calculate heat of adsorption $\Delta H°_{ads}$ and the standard entropy of adsorption $\Delta S°_{ads}$ by the expression:

$$\text{Log (K)} = (\Delta S°_{ads}/2.303R) - (\Delta H°_{ads}/2.303RT)$$

As tabulated in Table 5, the value for ΔH°_{ads} is coming out to be negative indicating that the process is exothermic in nature. Moreover, ΔH°_{ads} being less than 40 kJ/mol signifies that inhibitor is adsorbed on the metal surface through physisorption[36].

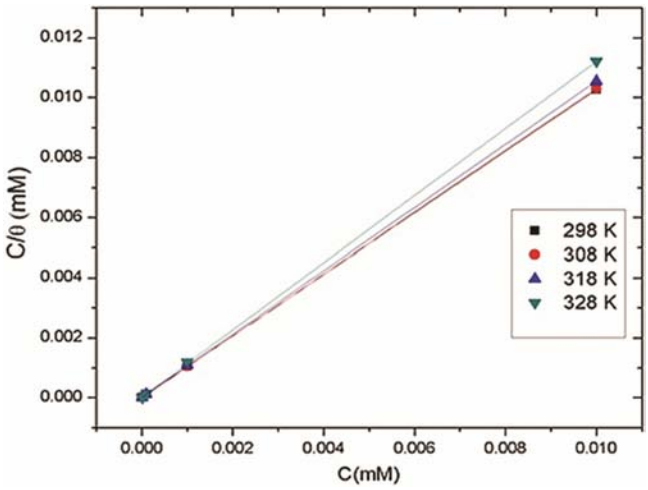

Fig. 5 — Langmuir Adsorption plots of DHQ on the Mild Steel surface in 0.5 M H_2SO_4

Table 4 — Electrochemical impedance parameters for mild steel in 0.5 M H_2SO_4 at various concentrations of DHQ at 298 K.

Conc. (M)	R_{ct} (Ω cm^{-2})	f_{max} (Hz)	C_{dl} (μF cm^{-2})	Θ_{EIS} (%)
10^{-2}	103.495	40.575	37.92	95.25
10^{-3}	67.846	29.118	80.60	92.76
10^{-4}	62.897	25.257	25.257	92.19
10^{-5}	49.287	19.200	168.27	90.04
0	4.907	2.165	14988.7	-

Table 5 — Thermodynamic parameters of adsorption for DHQ on mild steel surface.

Temperature (K)	K_{ads} x 10^5 M^{-1}	$-\Delta G^{\circ}_{ads}$ (kJ mol^{-1})	$-\Delta H^{\circ}_{ads}$ (kJ mol^{-1})	ΔS°_{ads} (JK^{-1} mol^{-1})
298	1.42	39.36	27.11	8.75
308	1.25	40.34		
318	1.00	41.06		
328	0.50	40.46		

Thus, from the values of $\Delta G°_{ads}$ and $\Delta H°_{ads}$ we can say that the inhibitor shows both chemisorption and physisorption i.e. cooperative adsorption[37]. The positive sign of $\Delta S°_{ads}$ could be due to the substitution mechanism which can be attributed to the increase in the solvent entropy and more positive water desorption entropy[38].

A plot of log (I_{corr}) versus 1/T in Fig. 7 was used to calculate the activation energy of the reaction at various concentrations of the inhibitor and in blank solution by the expression:

$$\text{Log}(I_{corr}) = \text{Log}A - (-E_a/2.303RT)$$

where, A = Arrhenius constant, E_a = activation energy of adsorption[39].

The slope of the straight line gives E_a and the intercept gives the value of A. As Table 6 signifies that the values of E_a are higher in presence of inhibitor than in the blank solution indicating that the energy barrier of corrosion reaction increases in presence of inhibitor without changing the mechanism of dissolution[12].

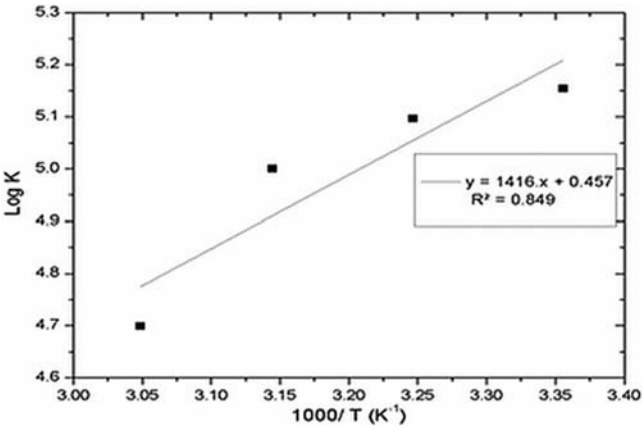

Fig. 6 — Plot of LogK v/s 1/T for DHQ on the mild steel surface in 0.5 M H_2SO_4

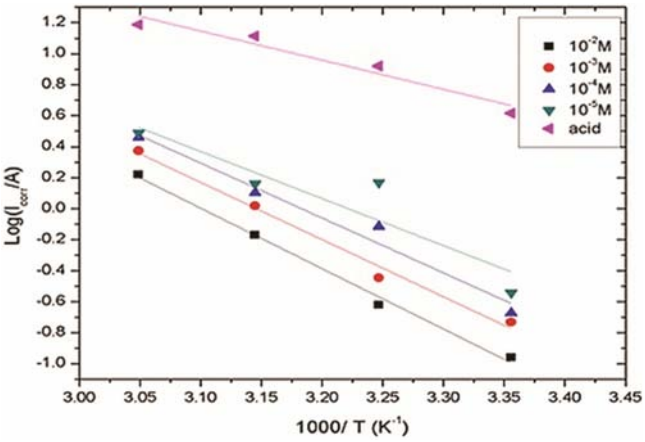

Fig. 7 — Plot of variation of log I_{corr} v/s 1/T for DHQ

Quantum chemical studies

The output produced by the program consists of the frontier orbital energies, total energy of the system, net atomic charges (calculated from the atomic orbital coefficients), dipole moment, and atomic orbital electron populations. The following quantum chemical descriptors were noted and tabulated in Table 7 for every inhibitor: the energy of the highest occupied molecular orbital (E_{HOMO}), the energy of the lowest unoccupied molecular orbital (E_{LUMO}), energy gap between frontier orbitals ($\Delta E = E_{LUMO} - E_{HOMO}$), the no. of electrons in the molecule, the binding energy of the inhibitor and the dipole moment (μ).

Figure 8 (A) shows the optimized structure of DHQ which suggest that DHQ is a planar molecule; and therefore the adsorption of DHQ on mild steel surface is uniform[16]. Figure 8 (B) is depicting 3-D isosurface of total charge density spread on the molecule. The atomic charge distribution can also be seen and it is observed that negative charge is concentrated on the N atoms and O atoms suggesting these to be the active sites for adsorption on the metal surface. The HOMO and the LUMO surfaces for the DHQ are given in Figs 8 (C) – 8 (D). HOMO and LUMO locations in the inhibitors are mostly distributed in the vicinity of the N atoms, O atoms and in the aromatic carbons indicating that interaction between metal surface and inhibitor takes place over nitrogen atoms, oxygen atoms and the π electrons.

The reactive abilities of the DHQ can be closely related to their frontier molecular orbitals i.e. highest occupied molecular orbital (HOMO) and the lowest

Table 6 — Parameters of Linear Regression between log I_{corr} and 1/T for DHQ.

Concentration (M)	log A	R^2	E (kJ mol^{-1})
10^{-2}	12.07	0.994	74.58
10^{-3}	11.60	0.989	70.59
10^{-4}	11.26	0.973	67.78
10^{-5}	9.783	0.850	58.15
0	6.79	0.945	34.92

Table 7 — Optimized parameters for DHQ

No. of electrons	Energy of HOMO ($kJmol^{-1}$)	Energy of LUMO ($kJmol^{-1}$)	ΔE ($kJmol^{-1}$)	Binding energy ($kJmol^{-1}$)	Dipole (debye)
60	-889.69	-70.43	819.26	-8548.75	1.409

unoccupied molecular orbital (LUMO)[40]. A higher HOMO energy (E_{HOMO}) of the molecule correlates to a higher electron-donating ability to an appropriate acceptor molecule with a low-energy empty molecular orbital[41]. As seen from Table 7 higher value of E_{HOMO} is obtained which indicates greater ease of offering electrons to the unoccupied d orbital of metallic iron and thus greater inhibition efficiency of the inhibitor due to enhanced adsorption[42]. Also the LUMO energy obtained is very low for DHQ indicating strong affinity of DHQ for iron. As it can be seen from Table 7, binding energy of DHQ is negative which indicates that DHQ is less prone to be split or broken apart[39]. The energy gap (ΔE) for the DHQ is very small which make the donation of electrons from the inhibitor molecule to the atoms on the surface of the metal very probable (i.e. soft- soft interaction) and thus increases the inhibition efficiency of the inhibitor[43].

The dipole moment (μ) is another indicator of the electronic distribution in a molecule and is one of the properties used to discuss and to rationalize the structure[44]. Authors could not find a significant relationship between the dipole moment values and inhibition efficiencies and there is a lack of agreement in the literature on the correlation of the both[45]. Some authors showed that an increase of the dipole moment leads to decrease of inhibition and vice versa, suggesting that lower values of the dipole moment will favor accumulation of the inhibitor in the surface layer whereas, some suggested the increase of the dipole moment can lead to increase of inhibition and vice versa, which could be related to the dipole–dipole interaction of molecules and metal surface[46].

Scanning electron microscope (SEM) analysis

The surface morphology of the mild steel in presence and absence of inhibitor was studied by scanning electron microscopy (SEM). Figures 9 (A) - (B) depicts the morphology of MS abraded and specimen after immersion for 24 h in 0.5 M H_2SO_4 solution. It can be clearly observed that the surface of MS in the blank (Fig. 9 (B)) is seriously damaged as compared to that before immersion (Fig. 9 (A)). Figure 9 (B) shows severe damage on mild steel surface due to metal dissolution in acid, which appeared to be started on grain boundaries which are active sites where dislocations and other lattice defects are accumulated and thus later spread to the wholesurface[47]. The SEM images (Figs 9 (C) – (D)) show the surface of mild steel surface immersed for 24 h in 0.5 M H_2SO_4 containing 10^{-2} and 10^{-5} M DHQ respectively. The SEM images revealed that the specimens immersed in the inhibitor solutions are in better conditions and are having smoother surface as compared to metal surface immersed in acid (Fig. 9 (B)) indicating that the DHQ molecules forms a organic film on the steel surface and hinder the dissolution of iron and thus reduces the rate of corrosion.

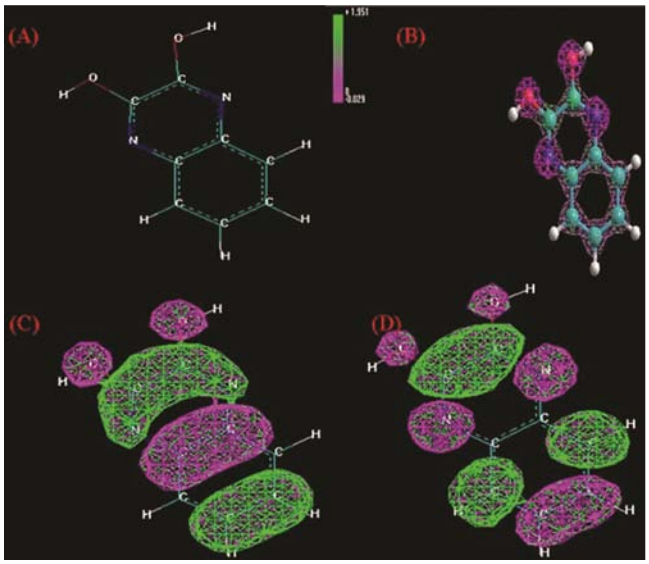

Fig. 8 — Structures made on Hyperchem for quantum chemical calculations: (A) Optimised structure of DHQ, (B) 3-D isosurface of total charge density, (C) HOMO of DHQ, (D) LUMO of DHQ

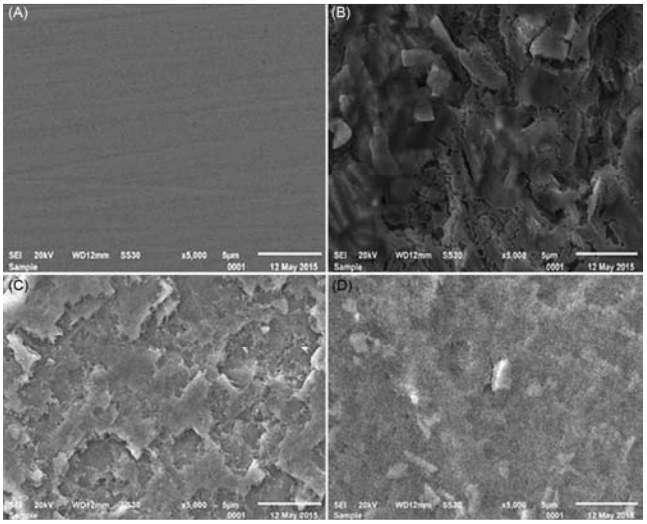

Fig. 9 — SEM micrographs of (A) Plain and Polished mild steel surface at 298 K, (B) Mild steel surface immersed for 24 h in 0.5 M H_2SO_4 , (C) 0.5 M H_2SO_4 with 10^{-2} M DHQ, (D) 10^{-5} M DHQ respectively.

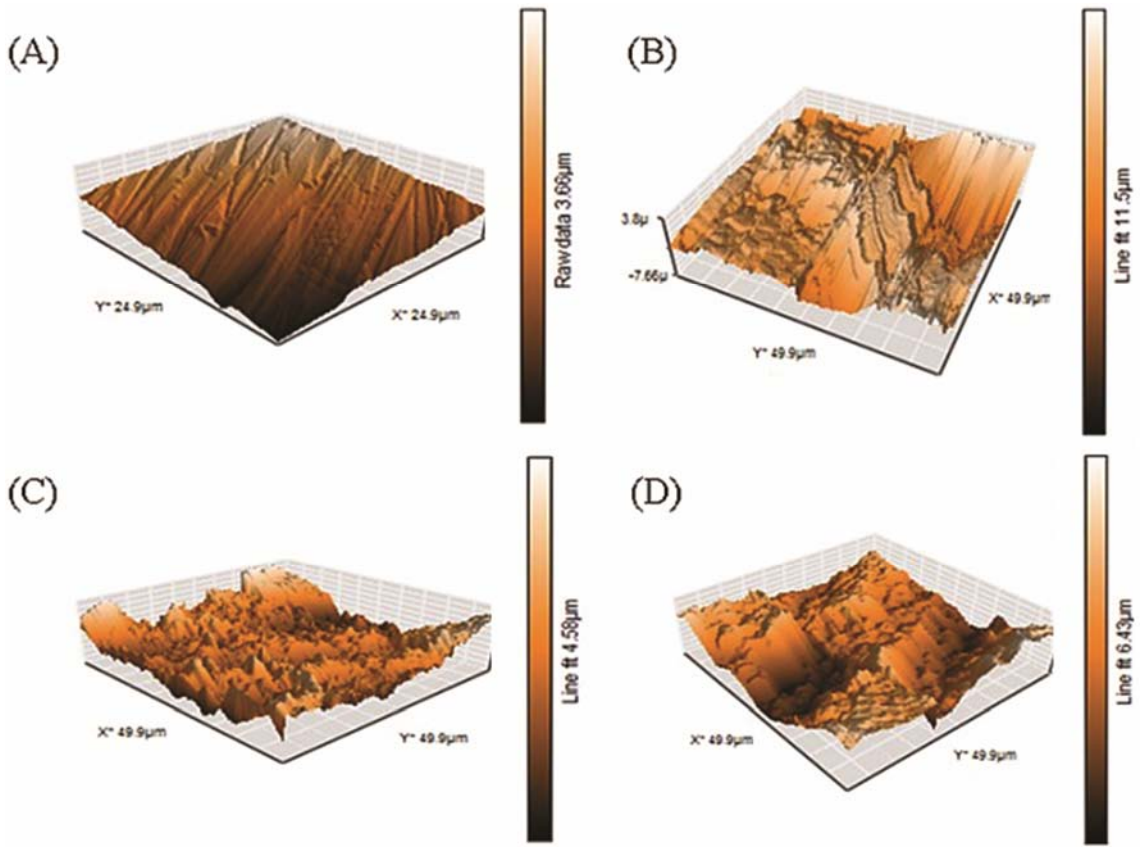

Fig. 10 — AFM images of mild steel surface (A) abraded, (B) immersed for 24 h in blank 0.5M H_2SO_4, (C) with 10^{-2} M DHQ, and D with 10^{-5} M DHQ.

Table 8 — The area and line roughness obtained from AFM of mild steel surfaces in absence and presence of DHQ at 298 K.

Roughness	Plain mild steel	Acid	10^{-2}M DHQ	10^{-5}M DHQ
Line, R_A (nm)	203.5	1228	252.1	382.8
Area, S_A (nm)	88.0	924.5	569.9	818.6

Atomic force microscope (AFM) analysis

AFM was employed for further study of metal/ solution interface as SEM does not provide topographic quantitative information[48-52]. The three dimensional (3D) AFM images of plain polishedmild steel surface before and after immersion for 24 h in 0.5 M H_2SO_4 solution at 298 K are shown in Figs 10 (A) – (B). It can be seen that the surface morphology of the corroded sample has been drastically changed after immersion in acid. Surface roughness examination (both line and area roughness results) of MS specimen immersed in acid clearly shows that have greater roughness with highly damaged surface due to direct aggressive attack of acid.

Figures 10 (C) – (D) depict the three dimensional (3D) AFM images of mild steel in 0.5 M H_2SO_4 in the presence of 10^{-2} and 10^{-5} M DHQ respectively. Close scrutiny of the reveals that the surface roughness due to aggressive corrosion attack is smoothened in the presence of the inhibitor. However, a more smooth surface morphology is obtained when specimen was dipped in higher concentration (10^{-2} M) of inhibitor as compared to lower concentration (10^{-5} M). Also, the line and area roughness data values listed in Table 8 depicts the same. This could be attributed to more adsorption of DHQ molecules on the mild steel surface in higher concentration.

Conclusion

The following conclusions can be drawn from the studies done:

1. The inhibition efficiency increases with increasing concentration of the inhibitor molecule but decreases with increase in temperature and the values obtained from weight loss, polarization and EIS methods are close to one another.
2. DHQ behaves as a mixed inhibitor for the mild steel corrosion in 0.5 M H_2SO_4.

3. The adsorption of inhibitor on surface of mild steel in 0.5 M H_2SO_4 followed Langmuir adsorption isotherm at all investigated temperatures.
4. Thermodynamic adsorption parameters (ΔG°_{ads}, ΔH°_{ads} and ΔS°_{ads}) show that the inhibitive action is due to comprehensive adsorption (physical and chemical adsorption) of DHQ on mild steel surface and the adsorption process is spontaneous in nature.
5. Quantum chemical calculation results showed that π electrons of aromatic rings and lone pair of electrons of 2 nitrogen atoms and 2 oxygen atoms are the active sites of the DHQ inhibitor.
6. SEM and AFM micrographs showed that in presence of acid mild steel surface is highly damaged and with the addition of inhibitor to the acid solution a smother surface is obtained due to the formation of a protective film on metal surface.

References

1 Yadav M, Behera D, Kumar S & Sinha R R, *Ind Eng Chem Res*, 52 (2013) 6318.
2 Amin M A & Ibrahim M M, *Corros Sci*, 53 (2012) 873.
3 Gopi D, Govindaraju K M & Kavitha L, *J Appl Electrochem*, 40 (2010) 1349.
4 Hegazy M A, Hasan A M, Emara M M, Bakr M F & Youssef A H, *Corros Sci*, 65 (2012) 67.
5 Xu F, Duan J, Zhang S & Hou B, *Mater Lett*, 62 (2008) 4072.
6 Bayoumi F M & Ghanem W A, *Mater Lett*, 59 (2005) 3806.
7 Anand B & Balasubramanian V, *Elixir Corros*, 37 (2011) 3832.
8 G Singh, *Corros Rev*, 27 (2009) 367.
9 Abbouda Y, Abourriche A, Saffaj T, Berrada M, Charrouf M, Bennamara A , Al Himidi N & Hannache H, *Mater Chem Phys*, 105 (2007) 1.
10 Zarrouk A, Zarrok H, Salghi R, Hammouti B, Al-Deyab S S, Touzani R, Bouachrine M, Warad I & Hadda T B, *Int J Electrochem Sci*, 7 (2012) 6353.
11 Fu J, Zang H, Wang Y, Li S, Chen T & Liu X, *Ind Eng Chem Res*, 51 (2012) 6377.
12 Chitra S, Parameswari K, Vidhya M, Kalishwari M & Selvaraj A, *Int J Electrochem Sci*, 6 (2011) 4593.
13 Zarrouk A, Dafali A, Hammouti B, Zarrok H, Boukhris S & Zertoubi M, *Int J Electrochem Sci*, 5 (2010) 46.
14 Obot I B & Obi-Egbedi N O, *Mater Chem Phys*, 122 (2010) 325.
15 Obot I B & Obi-Egbedi N O, *Corros Sci*, 52 (2010) 282.
16 Obot I B, Obi-Egbedi N O & Odozi N W, *Corros Sci*, 52 (2010) 923.
17 El Ouali I, Hammouti B, Aouniti A, Ramli Y, Azougagh M, Essassi E M & Bouachrine M, *J Mater Environ Sci*, 1 (2010) 1.
18 H Zarrok, A Zarrouk, R Salghi, Y Ramli, B Hammouti, S S Al-Deyab, E M Essassi & H Oudda, *Int J Electrochem Sci*, 7 (**2012**) 8958.
19 H Zarrok, A Zarrouk, R Salghi, M Assouag, B Hammouti, H Oudda, S Boukhris, S S Al Deyab & I Warad, *Der Pharmacia Lett*, 5 (**2013**) 43.
20 Yang L, *Techniques for Corrosion Monitoring*, Elsevier (2008).
21 Yadav M, Behera D & Sharma U, *Der ChemicaSinica*, 3 (2012) 262.
22 Zhang S, Tao Z, Liao S & Fengjing W, *Corros Sci*, 52 (2010) 3126.
23 Zheng X, Zhang S, Li W, Yin L, He J & Wua J, *Corros Sci*, 80 (2014) 383.
24 Yadav M, Behera D & Sharma U, *Arab J Chem*, 2012, doi: 10.1016/j.arabjc.2012.03.011.
25 Li W, He Q, Pei C & Hou B, *Electrochim Acta*, 52 (2007) 6386.
26 Sharma M, Chawla J & Singh G, *Indian J Chem Technol*, 16 (2009) 339.
27 Singh M R, Bhrara K & Singh G, *Port Electrochim Acta*, 26 (2008) 479.
28 Khaled K F, *Electrochim Acta*, 53 (2008) 3484.
29 Ahamad I & Quraishi M A, *Corros Sci*, 51 (2009) 2006.
30 Obot I B, Umoren S A, Gasem Z M, Suleiman R & El Ali B, *J Ind Eng Chem*, 21 (2015) 1328.
31 Abd El-Lateef H M, *Corros Sci*, 92 (2015) 104.
32 Bhrara K, Kim H & Singh G, *Corros Sci*, 50 (2008) 2747.
33 Prabhu R A, Venkatesha T V, Shanbhag A V, Kulkarni G M & Kalkhambkar R G, *Corros Sci*, 50 (2008) 3360.
34 Yilmaz N, Fitoz A, Ergun Ü, Emregül K C, *Corros Sci*, (2016) http://dx.doi.org/10.1016/j.corsci.2016.05.002.
35 Pavithra M K, Venkatesha T V, Kumar M K P & Tondan H C, *Corros Sc*i, 60 (2012) 104.
36 Noor E A & Al-Moubaraki A H, *Mater Chem Phys*, 110 (2008) 145.
37 Benabdellah M, Touzani R, Dafali A, Hammouti M & ElKadiri S, *Mater Lett*, 61 (2007) 1197.
38 Ahmed R A, *Orient J Chem*, 32 (2016) 295.
39 Bhrara K & Singh G, *Appl Surf Sci*, 253 (2006) 846.
40 Musa A Y, Jalgham R T T, Mohamad A B, *Corros Sci*, 56 (2012) 176.
41 Khaled K F, *J Solid State Electrochem*, 13 (2009) 1743.
42 Zhang D, An Z, Pan Q, Gao L & Zhou G, *Corros Sci*, 48 (2006) 1437.
43 Arslan T, Kandemirli F, Ebenso E E, Love I & Alemu H, *Corros Sci*, 51 (2009) 35.
44 Kikuchi O, *Quant. Struct Act Relat*, 6 (1987) 179.
45 Gece G & Bilgic S, *Corros Sci*, 51 (2009) 1876.
46 Behpour M, Ghoreishi S M, Khayatkashani M & Soltani N, *Corros Sci*, 53 (2011) 2489.
47 Olivares Xometl O, Likhanova N V, Dominguez Aguilar M A, Arce E, Dorantes H & Arellanes Lozada P, *Mater Chem Phys*, 110 (2008) 344.
48 Xu L, Fang H H P & Chan K, *J Electrochem Soc*, 146 (1999) 4455.
49 Meresht S E, Farahani T S & Neshati J, *Corros Sci*, 54 (2012) 36.
50 Sanchez J, Fullea J, Andrade C, Gaitero J J & Porro A, *Corros Sci*, 50 (2008) 1820.
51 Singh A K, Shukla S K, Quraishi M A & Ebenso E E, *J Taiwan Inst Chem Eng*, 43 (2012) 463.
52 Doner A, Solmaz R, Ozcan M & Kardas G, *Corros Sci*, 53 (2011) 2902.